White Rose Research Online

eprints@whiterose.ac.uk
https://eprints.whiterose.ac.uk
Universities of Leeds, Sheffield and York

Deposited via The University of Sheffield.

White Rose Research Online URL for this paper:
https://eprints.whiterose.ac.uk/id/eprint/163253/

Version: Published Version

Article:
Shulyak, V., Hayat, M.M. and Ng, J.S. (2020) Sensitivity calculations of high-speed optical receivers based on electron-APDs. Journal of Lightwave Technology, 38 (4). pp. 989-995. ISSN: 0733-8724

https://doi.org/10.1109/jlt.2019.2950804

Reuse
This article is distributed under the terms of the Creative Commons Attribution (CC BY) licence. This licence allows you to distribute, remix, tweak, and build upon the work, even commercially, as long as you credit the authors for the original work. More information and the full terms of the licence here: https://creativecommons.org/licenses/

Takedown
If you consider content in White Rose Research Online to be in breach of UK law, please notify us by emailing eprints@whiterose.ac.uk including the URL of the record and the reason for the withdrawal request.

UNIVERSITY OF LEEDS
University of Sheffield
UNIVERSITY of York

Sensitivity Calculations of High-Speed Optical Receivers Based on Electron-APDs

Vladimir Shulyak, Majeed M. Hayat, *Fellow, IEEE*, and Jo Shien Ng, *Member, IEEE*

***Abstract*—Sensitivity of high-speed optical receivers is heavily influenced by the performance of the optical detectors used in the receivers, the data rate, and the target bit-error-rate (BER). A simulation model for sensitivity of optical receivers based on electron-avalanche photodiodes (e-APDs) is presented. It allows for the optimization of avalanche width and operating voltage to achieve the optimum receiver sensitivity for given bit rate and target BER. The effects modelled include inter-symbol interference (ISI), various dark current components (tunnelling, diffusion, and generation), current impulse duration, avalanche gain, and amplifier's noise. The model was demonstrated through simulations of Indium Arsenide (InAs) e-APDs. For 10^{-12} target BER, the receiver's sensitivities were found to be −30.6, −22.7, −19.2, and −16.6 dBm, for 10, 25, 40, and 50 Gb/s data rate, respectively. Desirable avalanche properties of InAs e-APDs are counteracted by detrimental effects of high dark currents. Hence InAs e-APDs with lower dark currents are required to be more competitive with other optical detector technologies for high-speed optical receivers. The data reported in this article is available from the ORDA digital repository (DOI: 10.15131/shef.data.9959468).**

***Index Terms*—Avalanche photodiodes (APDs), bit-error rate (BER), dead space, impact ionization, indium Arsenide (InAs), intersymbol interference (ISI), noise, receiver sensitivity.**

I. Introduction

AVALANCHE photodiodes (APDs) are widely used optical detectors in the domain of high-speed optical receivers for long-haul optical communication systems. They offer high internal gain, which is the end result of numerous impact ionization events taking place within the APDs. When used in high-speed optical receivers, they reduce the dominance of noise from post-detection amplifier, thereby increasing the overall signal-to-noise ratio. In recent years there has been great interest in developing highly sensitive 25 and 40 Gbps receivers with acceptable bit-error rates.

The sensitivity of an optical receiver is defined as the minimum optical power required to reach a target bit-error rate (BER) - the probability of an error in bit-identification by the receiver. Several APD-related characteristics determine the performance of APD-based optical receivers, including (i) the excess noise factor; (ii) the stochastic avalanche duration, which increases with gain and decreases the APD's speed; (iii) the APD's dark current.

Analytical simulation models of APD-based receivers have been developed to determine their sensitivity [1]–[3]. These models assume both electrons and holes will impact ionize (indeed the case for important avalanche materials for optical receivers, such as InP and InAlAs), whereby the random avalanche buildup time within the APD is not deterministic. Hence, they cannot be applied without modification to an important sub-class of APDs known as an electron-APDs (e-APD). InAs [4] and HgCdTe [5] based APDs are examples of e-APDs. In these diodes, only the electrons undergo impact ionization, which leads to a unique impulse response function whose duration is deterministic and hence needs to be treated carefully in the receiver-sensitivity model. Unlike regular APDs, where each avalanche event has a different duration, an avalanche within an e-APD ends after two carrier transit times within the avalanche region, providing avalanche gain with little excess noise. Thus, eAPDs have potential in high-speed, low noise optical receivers.

In this paper we present a model that can be applied to any e-APD, capturing effects which include; inter-symbol interference (ISI), tunnelling current, diffusion current, generation current, avalanche pulse duration, avalanche gain, and amplifier noise. Sensitivity calculations obtained using our model for InAs e-APDs, which have excellent excess noise characteristics but relatively high dark currents, are also reported here to demonstrate the model's functionality.

II. Model Details

A. Review of the Model Reported in [2]

The model in this paper is based on the bit-error-rate (BER) model developed in [1] and [2], although there are some significant differences and modifications which need to be discussed. The unique impulse response of an e-APD means that many of the equations previously developed cannot be used, and a revision of the model must be carried out.

According to [1], the calculation of an analytical expression for the receiver sensitivity requires knowledge of analytical expressions for the stochastic photocurrent's mean and variance as a function of time following a single trigger of the avalanche process. (Such photocurrent is also referred to as the APD's stochastic impulse response function.) This task requires the

Manuscript received July 24, 2019; revised September 13, 2019; accepted October 7, 2019. Date of publication October 31, 2019; date of current version February 12, 2020. This work was supported by the Engineering and Physical Sciences Research Council under Grant EP/M508135/1. *(Corresponding author: Vladimir Shulyak.)*

V. Shulyak and J. S. Ng are with the Department of Electronic and Electrical, The University of Sheffield, Sheffield S3 7HQ, U.K. (e-mail: vshulyak1@shef.ac.uk; j.s.ng@shef.ac.uk).

M. M. Hayat is with the Department of Electrical and Computer Engineering, Marquette University, WI 53233 USA (e-mail: majeed.hayat@marquette.edu).

Digital Object Identifier 10.1109/JLT.2019.2950804

This work is licensed under a Creative Commons Attribution 4.0 License. For more information, see http://creativecommons.org/licenses/by/4.0/

adoption of a simplifying approximate exponential form for the mean and the autocorrelation functions. However, this approximation implicitly assumes a non-deterministic (and unbounded) duration of the mean and autocorrelation functions of time, an assumption that is justified when both electrons are capable of ionizing. Unfortunately, this assumption is incorrect for e-APDs because only electrons can impact ionize. The e-APD's stochastic impulse response function has a deterministic and finite duration. Hence, a new functional form for the mean and the auto correlation function of the stochastic impulse response is required for use in the framework described in [1]. In this paper we do just that.

We emphasize, however, that the limitation of the model in [2] arises only when an analytical formula for the receiver sensitivity is sought; the model in [2] remains valid for the numerical calculation of the sensitivity for electron APDs, though this would require significantly more computing resources to match the accuracy provided by a more analytical model. Although the analytical expressions for the mean and variance of the APDs stochastic impulse response function from [2] are no longer valid, the defining integrals for the mean and the variance are still valid and can still be used.

The formulae for the mean and variance of the ISI contributions ($\mu_{\mathrm{ISI,n}}$ and $\sigma^2_{\mathrm{ISI,n}}$) to receiver output from the nth past bit with duration T are given by equations (A3) and (A7) from [2]:

$$\mu_{\mathrm{ISI,n}} = \phi_0 \int_0^T \int_{-nT}^{-nT+T} \langle I_p(t-\tau)\rangle d\tau dt, \tag{1}$$

$$\sigma^2_{\mathrm{ISI,n}} = \phi_0 \int_0^T \int_0^T \int_{-nT}^{-nT+T} \times \langle I_p(\mu-\xi) I_p(\nu-\xi)\rangle d\xi d\mu d\nu, \tag{2}$$

where ϕ_0 is a constant photon flux present between times $-nT$ and $-nT+T$, while $\langle I_p(t)\rangle$ is the mean impulse response function.

When considering an arbitrary past bit pattern I_j of length L, the total contributions from all ISI terms, dark current mean and variance (μ_{dark} and σ^2_{dark}), and Johnson noise σ_J, the mean and variance for a "0" bit (μ_0 and σ_0^2) are given by

$$\mu_0(I_j) = \sum_{n=1}^{L} (a_n(I_j)\mu_{\mathrm{ISI},n}) + \mu_{\mathrm{dark}}, \tag{3}$$

and

$$\sigma_0^2(I_j) = \sum_{n=1}^{L} \left(a_n(I_j)\sigma^2_{\mathrm{ISI},n}\right) + \sigma^2_{\mathrm{dark}} + \sigma_J^2, \tag{4}$$

which are (9) and (11) in [2]. Here $a_n(I_j) = 1$ when the nth bit in the pattern I_j is a "1," and 0 otherwise. The mean and variance when the current bit is a "1" (μ_1 and σ_1^2) are then obtained by adding these contributions to $\mu_{\mathrm{ISI},0}$ and $\sigma^2_{\mathrm{ISI},0}$, with $n = 0$:

$$\mu_1(I_j) = \mu_0(I_j) + \mu_{\mathrm{ISI},0} \tag{5}$$

and

$$\sigma_1^2(I_j) = \sigma_0^2(I_j) + \sigma^2_{\mathrm{ISI},0} \tag{6}$$

Following [2], the pattern specific BER for $I_j = 1, \ldots, 2^L$ is given by

$$\mathrm{BER}(I_j) = \frac{1}{4}\left[\mathrm{erfc}\left(\frac{\theta - \mu_0(I_j)}{\sqrt{2}\sigma_0(I_j)}\right) + \mathrm{erfc}\left(\frac{\mu_1(I_j) - \theta}{\sqrt{2}\sigma_1(I_j)}\right)\right], \tag{7}$$

where θ is the decision threshold. The overall BER is then given by (14) from [2]:

$$\mathrm{BER} = \frac{1}{2^L}\sum_{j=1}^{2^L} \mathrm{BER}(I_j). \tag{8}$$

The threshold, θ, is adjusted to minimize the overall BER.

B. Modification of the Model for Optical Receivers based on e-APD

We use the asymptotic analytical mean impulse response (9) as seen in [6], developed by Saleh *et al.* as the basis of our model, which include dead-space and are valid for e-APDs [6]. In addition, we use the asymptotic expression

$$\langle I_p(t_1) I_p(t_2)\rangle \approx \frac{c'}{c^2}\langle I(t_1)\rangle\langle I(t_2)\rangle \tag{10}$$

for variance calculation, given by (41) in [6]. The terms in (9) and (10) are given by $1/v' = (1/v_e + 1/v_h)$, $\tau_e = d/v_e$, $\tau' = d/v'$, $T_e = w/v_e$, $T_f = w/v'$, d is dead-space, w is avalanche width, v_e and v_h are electron and hole drift velocities respectively. c and c' are constants defined by (23) and (24) in [6], calculated using

$$c = \frac{\alpha + \beta}{2\beta(\alpha d + \beta d + 1)} \tag{11}$$

and

$$c' = \frac{c^2(\beta/\alpha + 1)^2}{1 + 2\beta/\alpha - (\beta/\alpha)^2}, \tag{12}$$

where α is the impact ionization coefficient for electrons that have already travelled a distance of dead-space d, and β is derived from the so-called scaled Malthusian parameter, solution

$$\langle I_p(t)\rangle = \begin{cases} \frac{qv_e}{w} & \text{for } 0 \le t \le \tau_e \\ \frac{cq}{w}\left((v_e + v_h)\left(e^{\beta v_e t} - e^{\beta d}\right) + \frac{v_e}{c}\right) & \text{for } \tau_e < t \le \tau' \\ \frac{cq}{w}\left((v_e + v_h)\, e^{\beta v_e t} - v_h e^{\beta v' t} - v_e e^{\beta d} + \frac{v_e}{c}\right) & \text{for } \tau' < t \le T_e \\ \frac{cq}{w} v_h \left(e^{\beta w} - e^{\beta v' t}\right) & \text{for } T_e < t \le T_f \\ 0 & \text{otherwise} \end{cases} \tag{9}$$

to the equation

$$2e^{-\alpha d} - \beta/\alpha = 1. \tag{13}$$

This asymptotic result is valid when $w \gg d$. Validation of these formulae for estimating gain and excess noise was recently performed by Jamil *et al.*, who were able to accurately predict these characteristics in InAs APDs with avalanche widths as low as 500 nm [7].

Using an analytical expression for mean and variance as a function of time allows for reduced computation time, in contrast to using a Random Path Length (RPL) model to generate the mean impulse response [8]. As in [2], we consider the past bit stream as well as the state of the present bit. A crucial difference is that we are able to determine the required bit stream length, L, precisely with L defined analytically using

$$L = \left\lceil \frac{T_f}{T} \right\rceil, \tag{14}$$

where the brackets represent the ceiling function. Since L is known analytically (and depends on w/v'), it is possible to capture the full contribution to mean and variance from ISI (previously the maximum L had to be deduced through trial and error). This also allows for the precise calculation of dark current components on the current detection bit for an impulse with duration T_f, using modified forms of (1) and (2);

$$\mu_{\text{dark}} = \phi_{\text{dark}} \int_0^T \int_{-T_f}^0 \langle I_p(t-\tau)\rangle d\tau dt \tag{15}$$

and

$$\sigma^2_{\text{dark}} = \phi_{\text{dark}} \int_0^T \int_0^T \int_{-T_f}^0 \times \langle I_p(\mu-\xi) I_p(\nu-\xi)\rangle d\xi d\mu d\nu \tag{16}$$

where ϕ_{dark} is the number of charges caused by dark currents; it is given by

$$\phi_{\text{dark}} = \frac{I_{\text{tunn}} + I_{\text{bulk}}}{q}, \tag{17}$$

where q is electron charge, I_{tunn} is the tunneling current, and I_{bulk} is combined diffusion and generation currents. I_{bulk} is given by experimental value of $J_0 A$, where J_0 is bulk dark current density and A is device area [9]. I_{tunn} is given by [10]

$$I_{\text{tunn}} = \frac{(2m^*)^{0.5} q^3 F V A}{h^2 E_g^{0.5}} \exp\left(-\frac{2\pi\sigma_T (m^*)^{0.5} E_g^{1.5}}{qhF}\right), \tag{18}$$

where m^* is the effective electron mass, F is electric field, V is voltage, A is device area, h is Planck's constant, k is Boltzmann's constant, E_g is band-gap, and σ_T is the tunnelling parameter.

After substitution of (15) and (16) into (3) and (4), the pattern specific and overall BER can be calculated. The integrals are evaluated using the QUADPACK numerical method [11].

TABLE I
MODEL PARAMETERS FOR INAS E-APDS

Parameter		Value	Ref.
Temperature T (K)		293	
Device diameter (μm)		20.0	
TIA bandwidth (GHz)	10 Gb/s	8.0	[12]
	25 Gb/s	16.0	[13]
	40 Gb/s	35.0	[14]
	50 Gb/s	32.0	[15]
TIA noise current ($\text{pA}/\sqrt{\text{Hz}}$)	10 Gb/s	6.5	[12]
	25 Gb/s	15.0	[13]
	40 Gb/s	14.0	[14]
	50 Gb/s	23.0	[15]
Electron effective mass m^*		0.023 m_0	[16]
Bandgap E_g (eV)		0.356	[4]
Tunneling parameter σ_T		1.16	[17]
Bulk dark current density J_0 (A/m^2)		68.8	[9]

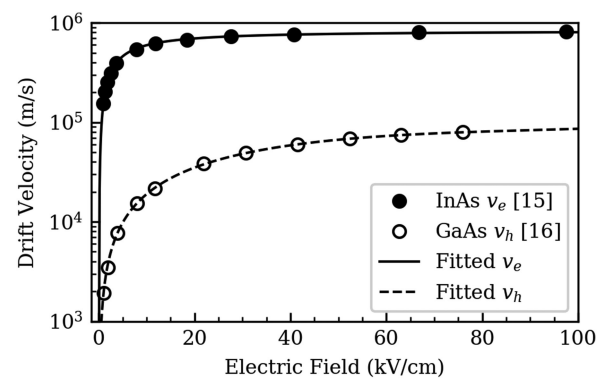

Fig. 1. Simulated electron drift velocity of InAs [18] and experimental hole drift velocity of GaAs [19]. Fittings (lines) to these data are used in our simulations of optical receivers based on InAs e-APDs.

III. RESULTS

A. Model Parameters for InAs e-APDs

Some of the material-dependent parameter values used for our room temperature InAs e-APD simulations are summarized in Table I. In the simulations, the Johnson noise due to the transimpedance amplifier (TIA) was given by $\sigma_J = (\sqrt{B_{\text{TIA}} i_n^2}/q)(1/R_b)$, where i_n and B_{TIA} are the input noise current density and bandwidth of a typical TIA at a given bit rate R_b [2]. For impact ionization, we used the electron ionization coefficient from [4] and assumed that holes do not impact ionize. For electron drift velocity, due a lack of experimental reports at electric fields above 10 kV/cm (the relevant fields for impact ionization in InAs) [20], our fitting to simulated values from [18], as shown in Fig. 1, was used. Similarly, we used GaAs hole drift velocity from [19] (also plotted in Fig. 1) for holes in InAs e-APDs, since room temperature experimental hole mobilities in InAs are similar to those of GaAs (460 and 400 cm^2/Vs, respectively [21]). With these parameters, an example mean impulse response is calculated and shown in Fig. 2. Overall dark current is calculated based on experimental bulk dark

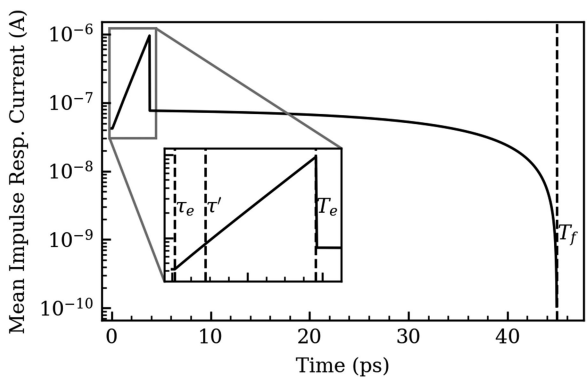

Fig. 2. Calculated mean impulse response for an InAs e-APD with $w = 3.0$ μm reverse biased at 18 V. The different stages of the mean impulse response function are indicated by the dashed lines in the figure.

current [9], tunneling current [17], and avalanche gain (which can be calculated from impact ionization coefficients [4]). In our calculations, the ratio of the dead-space to the avalanche width ranges from 0.016 to 0.037 at the operational gains; hence, the assumption is valid, which justifies the use of the asymptotic approximation in (9) and (10) in all of the results reported in this paper.

Using these parameters and the equations discussed in Section II, calculations of overall system's sensitivity for target BER ranging from 10^{-12} to 10^{-3} and 1550 nm wavelength were performed for InAs e-APDs. The simulation conditions covered a range of avalanche widths at data rates of 10, 25 and 40 Gbit/s. The electric field profiles of the e-APDs were assumed to be constant across the avalanche region, with negligible depletion into the p and n regions. For a given avalanche width and data rate, a full set of field-dependent parameters was calculated for each reverse voltage. The minimum avalanche widths used exceeded 1 μm to ensure approximations related to impulse response currents are valid.

B. Effects of Gain, Bandwidth, and Dark Current

For a given e-APD avalanche width, as the reverse voltage increases, there are changes in gain, bandwidth, and dark current, all of which contribute to the final BER values. This is illustrated in Fig. 3, which plots the results from the $w = 3.0$ μm (optimal for 10 Gbit/s operation) InAs e-APD as functions of reverse voltage, for a 10 Gbit/s data rate and 10^{-12} target BER. As reverse voltage increases, gain and bandwidth increase, which together improve the sensitivity. On the other hand, the bulk dark current increases due to increased gain and/or tunneling current (depending on the reverse voltage), limiting the beneficial effect of gain on sensitivity somewhat. Eventually, rising tunneling current causes the sensitivity to degrade. This trend is consistent with observations from earlier BER simulations for other avalanche materials [2], [3], although the magnitude of tunneling current is more pronounced in our results for InAs e-APDs due to the material's small, direct bandgap. Indeed, to avoid significant tunneling current, it is not desirable to use an InAs e-APD with $w < 1$ μm.

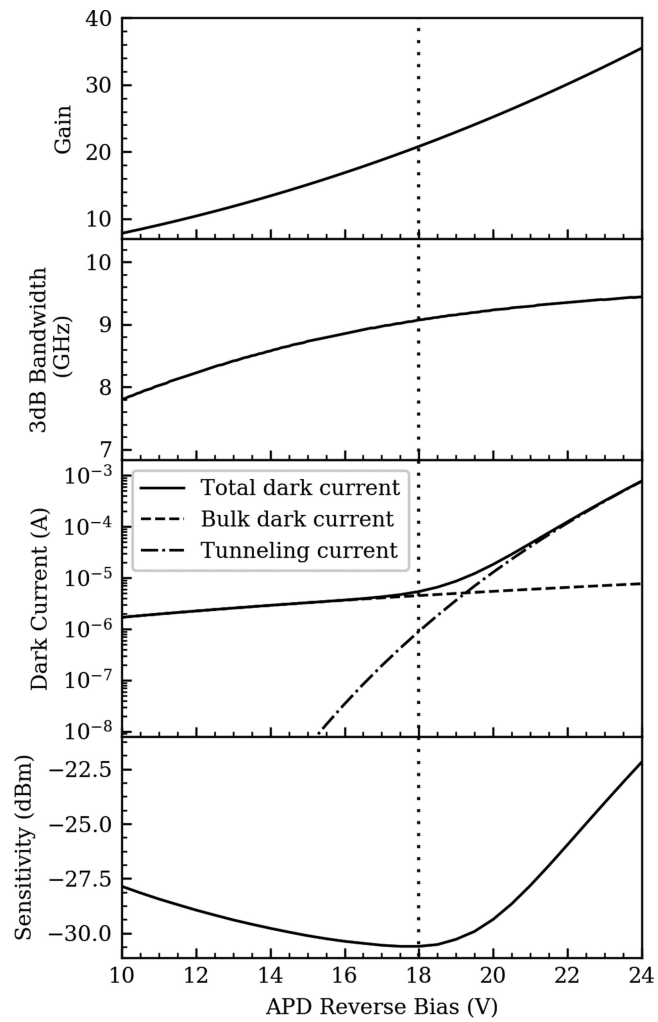

Fig. 3. Gain, 3 dB bandwidth, dark current, and sensitivity simulation data for a $w = 3.0$ μm InAs e-APD operated at 10 Gb/s bit rate and 1×10^{-12} target BER. Its optimal operating voltage (-18 V) is indicated by the dotted line.

Observing Fig. 3, the 3 dB bandwidth does not decrease with increasing gain in the $w = 3.0$ μm e-APD thanks to a lack of hole impact ionization, thus avoiding the usual gain-bandwidth product limitation in other APDs [22]. This is supported by results of 3 dB bandwidth versus gain from two other e-APDs ($w = 1.6$ and 2.3 μm), as shown in Fig. 4. The gradual increase in the bandwidth values at low gains is caused by the field dependence of drift velocities assumed for InAs e-APDs.

C. Sensitivity at Different Avalanche Widths and Bit Rates

Simulated characteristics of sensitivity versus reverse voltage for different InAs e-APDs ($w = 2.5$, 3.0, 3.5 and 4.0 μm) are compared in Fig. 5 for 10 Gb/s data rate and 10^{-12} target BER. The optimal avalanche region width for an InAs e-APD for these conditions can be found at the sensitivity minimum. As avalanche width increases, the e-APD is able to reach a higher operating voltage before sensitivity begins to degrade. This is due to the combined beneficial effects of larger gain and reduced tunneling current, for a given reverse voltage. At large

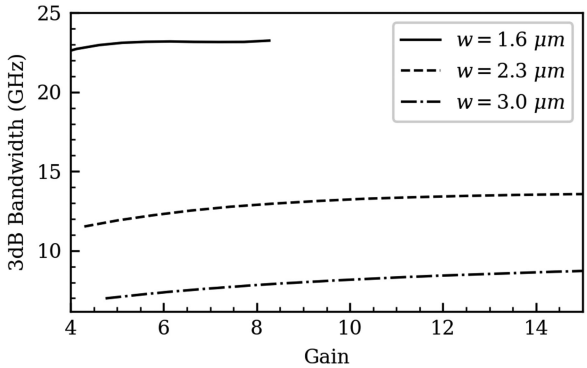

Fig. 4. Bandwidth versus avalanche gain characteristics of three simulated InAs e-APDs. Unlike other materials, bandwidth does not decrease with gain.

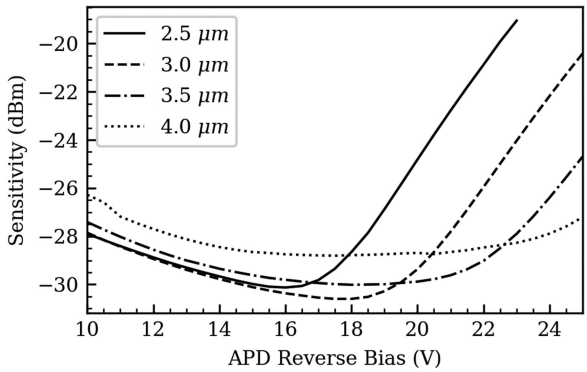

Fig. 5. Sensitivity versus APD reverse bias as function of avalanche width for 10 Gb/s data rate and 1×10^{-12} target BER.

avalanche widths, these benefits are however outweighed by the reduced bandwidth (longer impulse duration) and the increased intersymbol interference.

As previously mentioned, since in an e-APD gain is no longer limited by bandwidth, there is no single optimum operating gain across widths, unlike in InP and InAlAs APDs [2], [3]. This, compounded with the shorter impulse duration, means that optimum operating widths are much larger than for regular APDs. This demonstrates how design considerations for high speed, highly sensitive e-APDs differ from other diodes, and is a key contribution of this work.

Results of sensitivity versus avalanche width for data rate of 10, 25, and 40 Gb/s (all at a BER of 10^{-12}) are compared in Fig. 6. This yields a minimum sensitivity of -30.60, -22.74, and -19.17 dBm for 10, 25, and 40 Gb/s operation, respectively. The corresponding optimal avalanche widths are 3.0, 2.3 and 1.5 μm. In general, avalanche width of e-APDs should be maximized (subject to the bandwidth constraint) to maximize avalanche gains and avoid significant tunneling current. At higher data rates, more stringent bandwidth constraint causes smaller optimal avalanche width for e-APDs, in order to achieve the best possible sensitivity.

Calculations were also performed to yield plots of target BER versus sensitivity for InAs e-APDs detecting 1550 and 1310 nm wavelength photons, as shown in Fig. 7(a) and (b), respectively. The results are for data rates of 10, 25 and 40 Gb/s.

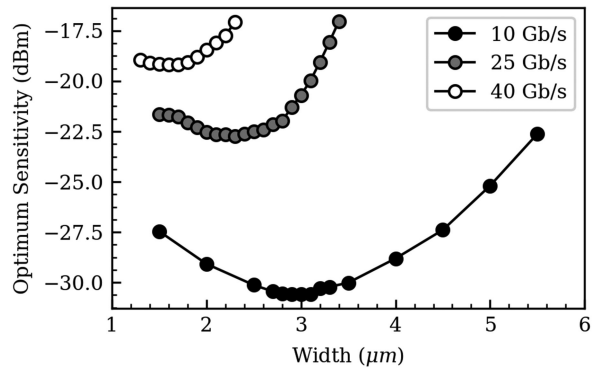

Fig. 6. Gain-optimized sensitivity for each simulated avalanche width for a 1×10^{-12} target BER.

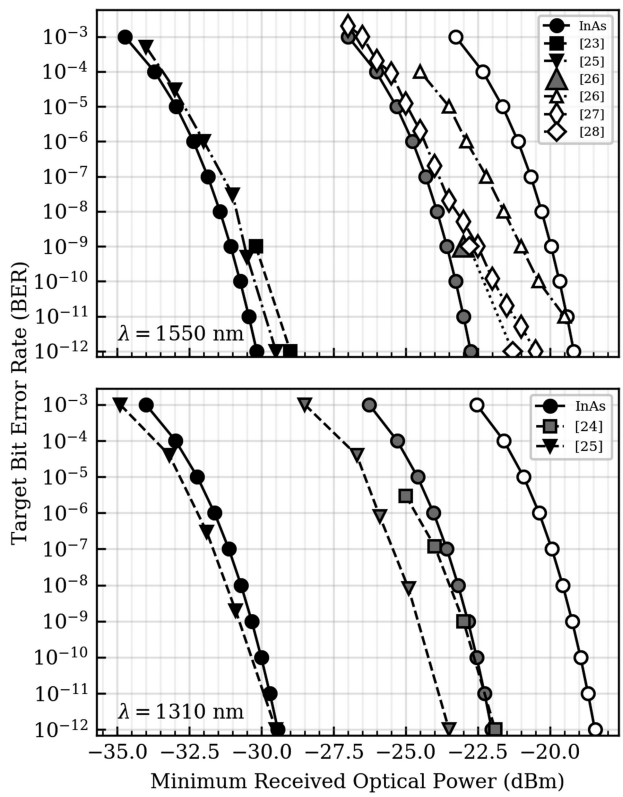

Fig. 7. Variable target BER versus optimum sensitivity for InAs APD-TIA combinations for (a) 1550 nm and (b) 1310 nm wavelength operation. The data rates are 10 (black circles, $w = 3$ μm), 25 (grey circles, $w = 2.3$ μm), and 40 Gb/s (open circles, $w = 1.5$ μm). Other high speed detector systems (other symbols, using identical color scheme for the different bit-rates), such as InAlAs APDs [23], [24], Ge/Si APD [25], and SOA-PIN combinations [26]–[28] are included for comparison.

Relevant reports of optical receivers based on other APD technologies [23]–[25] or Semiconductor Optical Amplifier (SOA)-PIN combinations [26]–[28] are included for comparison. For 1550 nm wavelength systems, at 10 and 25 Gb/s data rate, the InAs e-APDs compare favorably with receivers based on InAlAs APDs [23], [24]. At 40 Gbps, the performance of InAs eAPDs is worse than those of SOA-PIN from [26]–[28], except at more demanding BER. Note that optical receivers based on Ge/Si

APDs at 25 Gb/s are absent in Fig. 7(a) because their values at 1550 nm wavelength (-16 dBm at 1×10^{-12} BER [25]) are out of range.

Observing Fig. 7(b), for 1310 nm wavelength systems, optical receivers based on Ge/Si APDs generally provide better sensitivity than InAs e-APDs. It is however emphasized that these comparisons will evolve depending on the future performance of each of these technologies. For InAs e-APDs, reducing their tunneling current density through engineering of a more parabolic tunneling barrier shape, and reducing their bulk dark current density could lead to improved performance for optical receivers.

To test the effects of various dark current components on sensitivity values, a separate set of calculations were carried using $I_{\mathrm{bulk}} = 0$ (retaining I_{tunn} with $\sigma_T = 1.16$). There was no significant improvement in sensitivity values for the optimum avalanche widths and voltages, although the sensitivities at non-optimum avalanche widths do improve by up to 0.5 dBm for 25 Gbps bit rates. Further simulations were performed using I_{tunn} with $\sigma_T = 1.88$, which corresponds to a parabolic tunneling barrier rather than a triangular barrier when $\sigma_T = 1.16$ [10]. This showed a marked improvement in optimum sensitivities with the 40 Gbps value becoming -20.6 dBm. It is important to note, however, that engineering such a barrier would require a graded doping profile through the avalanche region, which would negatively impact on the magnitude of avalanche gain, the effects of which were not modelled in these additional simulations. There may be a middle ground to be explored which would lead to improved sensitivity overall. Simulations were also performed at 50 Gbps for key target BERs of 10^{-3}, 10^{-9}, and 10^{-12}, with resulting optimum sensitivities of -20.6, -17.3, and -16.6 dBm ($w = 1.4$ μm) for 1550 nm operation.

IV. Conclusion

A model for sensitivity of optical receivers based on e-APDs, in which only the electrons contribute to impact ionization, has been presented. The new model was demonstrated through optical receiver's sensitivity calculations of room temperature InAs e-APDs, using current performance parameters of InAs e-APDs. From the calculation results, the best sensitivity values for InAs e-APDs are -30.6, -22.7, -19.2, and -16.6 dBm, at 10, 25, 40, and 50 Gb/s data rate, respectively. Although InAs e-APDs offer improved sensitivity compared to InAlAs APDs at 10 and 25 Gb/s, they are not as competitive as SOA-PIN combinations at 40 Gb/s for 1550 nm wavelength systems. For 1310 nm systems, the Ge/Si APDs offer better sensitivity than InAs e-APDs. Thus InAs e-APDs will need to have lower dark currents for a more optimized performance in high-speed optical receivers.

References

[1] P. Sun, M. Hayat, B. Saleh, and M. Teich, "Statistical correlation of gain and buildup time in APDs and its effects on receiver performance," *J. Lightw. Technol.*, vol. 24, no. 2, pp. 755–768, Feb. 2006.

[2] D. S. G. Ong, J. S. Ng, M. M. Hayat, P. Sun, and J. David, "Optimization of InP APDs for high-speed lightwave systems," *J. Lightw. Technol.*, vol. 27, no. 15, pp. 3294–3302, Aug. 2009.

[3] D. S. G. Ong, M. M. Hayat, J. P. R. David, and J. S. Ng, "Sensitivity of high-speed lightwave system receivers using InAlAs avalanche photodiodes," *IEEE Photon. Technol. Lett.*, vol. 23, no. 4, pp. 233–235, Feb. 2011.

[4] A. R. J. Marshall, J. P. R. David, and C. H. Tan, "Impact ionization in InAs electron avalanche photodiodes," *IEEE Trans. Electron Devices*, vol. 57, no. 10, pp. 2631–2638, Oct. 2010.

[5] J. Beck *et al.*"The HgCdTe electron avalanche photodiode," *J. Electron. Mater.*, vol. 35, no. 6, pp. 1166–1173, 2006.

[6] B. E. A. Saleh, M. M. Hayat, and M. C. Teich, "Effect of dead space on the excess noise factor and time response of avalanche photodiodes," *IEEE Trans. Electron Devices*, vol. 37, no. 9, pp. 1976–1984, Sep. 1990.

[7] E. Jamil, M. M. Hayat, and G. A. Keeler, "Analytical formulas for mean gain and excess noise factor in InAs avalanche photodiodes," *IEEE Trans. Electron Devices*, vol. 65, no. 2, pp. 610–614, Feb. 2018.

[8] J. S. Ng *et al.*, "Effect of dead space on avalanche speed," *IEEE Trans. Electron Devices*, vol. 49, no. 4, pp. 544–549, Apr. 2002.

[9] P. J. Ker, A. R. J. Marshall, A. B. Krysa, J. P. R. David, and C. H. Tan, "Temperature dependence of leakage current in InAs avalanche photodiodes," *IEEE J. Quantum Electron.*, vol. 47, no. 8, pp. 1123–1128, Aug. 2011.

[10] S. R. Forrest, M. DiDomenico, R. G. Smith, and H. J. Stocker, "Evidence for tunneling in reverse-biased III-V photodetector diodes," *Appl. Phys. Lett.*, vol. 36, no. 7, pp. 580–582, 1980.

[11] R Piessens, *Quadpack: A Subroutine Package for Automatic Integration*. Berlin, Germany: Springer-Verlag, 1983.

[12] H. Ikeda, T. Ohshima, M. Tsunotani, T. Ichioka, and T. Kimura, "An auto-gain control transimpedance amplifier with low noise and wide input dynamic range for 10-Gb/s optical communication systems," *IEEE J. Solid-State Circuits*, vol. 36, no. 9, pp. 1303–1308, Sep. 2001.

[13] ADSANTEC, "ASNT6123 25 Gbps Dual Transimpedance Amplifier," Jan. 2010.

[14] S.-T. Chou, S.-H. Huang, Z.-H. Hon, and W.-Z. Chen, "A 40 Gbps optical receiver analog front-end in 65 nm CMOS," in *Proc. IEEE Int. Symp. Circuits Syst.*, May 2012, pp. 1736–1739.

[15] ADSANTEC, *ASNT6122-BD 50 Gbps Linear/Limiting TIA*. May 2017.

[16] W. Nakwaski, "Effective masses of electrons and heavy holes in GaAs, InAs, AlAs and their ternary compounds," *Physica B, Condensed Matter*, vol. 210, pp. 1–25, Apr. 1995.

[17] A. R. Marshall, "The InAs electron avalanche photodiode and the influence of thin avalanche photodiodes on receiver sensitivity," Ph.D. Thesis, Univ. Sheffield, Sheffield, U.K., 2009.

[18] K. Brennan and K. Hess, "High field transport in GaAs, InP and InAs," *Solid-State Electron.*, vol. 27, no. 4, pp. 347–357, 1984.

[19] V. L. Dalal, "Hole velocity in *p* -GaAs," *Appl. Phys. Lett.*, vol. 16, pp. 489–491, Jun. 1970.

[20] M. V. Fischetti, "Monte Carlo simulation of transport in technologically significant semiconductors of the diamond and zinc-blende structures. I. Homogeneous transport," *IEEE Trans. Electron Devices*, vol. 38, no. 3, pp. 634–649, May 1991.

[21] S. M. Sze and K. K. Ng, *Physics of Semiconductor Devices*. 3rd ed. Hoboken, NJ, USA: Wiley-Interscience, 2007.

[22] R. B. Emmons, "Avalanche-photodiode frequency response," *J. Appl. Phys.*, vol. 38, pp. 3705–3714, Aug. 1967.

[23] K. Shiba, T. Nakata, T. Takeuchi, T. Sasaki, and K. Makita, "10 Gbit/s asymmetric waveguide APD with high sensitivity of -30 dBm," *Electron. Lett.*, vol. 42, no. 20, pp. 1177–1178, 2006.

[24] M. Nada, Y. Muramoto, H. Yokoyama, T. Ishibashi, and S. Kodama, "High-sensitivity 25 Gbit/s avalanche photodiode receiver optical sub-assembly for 40 km transmission," *Electron. Lett.*, vol. 48, no. 13, pp. 777–778, 2012.

[25] Z. Huang *et al.*, "25 Gbps low-voltage waveguide SiGe avalanche photodiode," *Optica*, vol. 3, pp. 793–798, Aug. 2016.

[26] C. Caillaud *et al.*, "Integrated SOA-PIN detector for high-speed short reach applications," *J. Lightw. Technol.*, vol. 33, pp. 1596–1601, Apr. 2015.

[27] P. Angelini *et al.*, "Record -22.5-dBm sensitivity SOA-PIN-TIA photoreceiver module for 40-Gb/s applications," *IEEE Photon. Technol. Lett.*, vol. 27, no. 19, pp. 2027–2030, Oct. 2015.

[28] S. Takashima, H. Nakagawa, S. Kim, F. Goto, M. Okayasu, and H. Inoue, "40-Gbit/s receiver with -21 dBm sensitivity employing filterless semiconductor optical amplifier," in *Proc. OFC Opt. Fiber Commun. Conf.*, vol. 2, Mar. 2003, pp. 471–472.

Vladimir Shulyak received the M.Phys. degree in physics from the University of Sheffield, Sheffield, U.K., in 2015.

He is currently working toward the Ph.D. degree in electronic engineering with the Department of Electronic and Electrical Engineering, University of Sheffield. His research interests include Geiger-mode avalanche photodiodes, avalanche photodiode based optical receivers, avalanche photodiode structure design, and diode characterization.

Majeed M. Hayat (S'89–M'92–SM'00–F'14) received the B.S. degree (*summa cum laude*) in electrical engineering from the University of the Pacific, Stockton, CA, USA, in 1985, and the M.S. and the Ph.D. degrees in electrical and computer engineering from the University of Wisconsin-Madison, Madison, WI, USA, in 1988 and 1992, respectively. He is currently a Professor and Department Chair of electrical and computer engineering with Marquette University, Milwaukee, WI, USA.

He has authored or co-authored nearly 110 peer-reviewed journal articles and 130 conference papers (more than 5000 citations, H-Index: 36). He has 14 issued patents, five of which have been licensed. His research activities cover a broad range of topics including avalanche photodiodes, high-speed optical communication, signal processing for synthetic aperture radar, data-compressive algorithms for spectral sensing and imaging, networked computing, and interdependent networks and cyberphysical systems with applications to smart grids.

Dr. Hayat was an Associate Editor of *Optics Express* from 2004 to 2009, the Chair of the Topical Subcommittee of the IEEE Photonics Society from 2009 to 2013, and Associate Editor of the IEEE TRANSACTIONS ON PARALLEL AND DISTRIBUTED COMPUTING from 2014 to 2018. He is recipient of the NSF Early Faculty Career Award (1998). Dr. Hayat is a Fellow of SPIE and OSA.

Jo Shien Ng (M'99) received the B.Eng. and Ph.D. degrees in electronic engineering from the University of Sheffield, Sheffield, U.K., in 1999 and 2003, respectively.

She is currently a Professor of semiconductor devices with the Department of Electronic and Electrical Engineering, University of Sheffield. She was a Royal Society Research Fellow based in the same department between 2006 and 2016. Her research interests include avalanche photodiodes, Geigermode avalanche photodiodes, and material characterization.